

Musculoskeletal Radiology / Radiologies musculo-squelettique

Imaging Evaluation of Complications of Hip Arthroplasty: Review of Current Concepts and Imaging Findings

Omer Awan, MD^{a,b,*}, Lina Chen, MD^b, Charles S. Resnik, MD^b

^aDepartment of Radiology, Beth Israel Deaconess Medical Center, Harvard Medical School, Boston, Massachusetts, USA
^bDepartment of Diagnostic Radiology and Nuclear Medicine, University of Maryland Medical Center, Baltimore, Maryland, USA

Abstract

Total hip arthroplasty has evolved along with improvements in component materials and design. The radiologist must accurately diagnose associated complications with imaging methods and stay informed about newer complications associated with innovations in surgical technique, prosthetic design, and novel materials. This pictorial essay presents clinical and imaging correlation of modern hip arthroplasty complications, with an emphasis on the most common complications of instability, aseptic loosening, and infection as well as those complications associated with contemporary metal-on-metal arthroplasty.

Résumé

L'arthroplastie totale de la hanche a progressé, au même rythme que les matériaux et que la conception des prothèses utilisées. Le radiologiste doit s'appuyer sur les méthodes d'imagerie pour diagnostiquer avec exactitude les complications associées et être au fait des nouvelles complications découlant des innovations sur le plan des techniques chirurgicales, de la conception des prothèses et des matériaux novateurs. Cette revue iconographique met en relation la clinique et l'imagerie propre aux complications contemporaines de l'arthroplastie de la hanche, en portant une attention particulière aux complications les plus fréquentes, notamment l'instabilité, le descellement aseptique et l'infection, ainsi que les complications associées aux arthroplasties contemporaines utilisant des prothèses avec couple de frottement métal-métal.

© 2013 Canadian Association of Radiologists. All rights reserved.

Key Words: Hip arthroplasty; Complications; Radiography; Computed tomography; Magnetic resonance imaging

Total hip arthroplasty (THA) is among the most successful procedures for relieving pain and improving function in the arthritic hip [1]. The reported incidence of complications ranges from 6.5%-7.6 % [2]. Radiologists must be knowledgeable of the diverse imaging appearances of these complications, understand the advantage and limitation of each imaging modality, and provide cost-effective evaluation for postoperative THA. In this article, we will describe metal artifact reduction techniques for computed tomography (CT) and magnetic resonance (MR) imaging and illustrate the imaging appearance of the most common early and late complications after modern THA.

Imaging remains the cornerstone of follow-up for patients with THA. Radiographs are essential for the initial assessment of postoperative complications. Common early postoperative complications, such as hardware dislocation or malposition, and late complications, including heterotopic ossification and periprosthetic fracture, can be demonstrated on plain radiographs. However, sensitivity of radiography for early septic and aseptic loosening and soft-tissue pathology is limited. Joint aspiration and arthrography are useful for evaluating infection and demonstrating sinus tract and communicating periarticular fluid collections. Ultrasound and nuclear medicine imaging provide further complement in evaluating infection and fluid collections.

Beam-hardening artifact in CT and susceptibility artifact in MR imaging have limited the application of these modalities in patients after THA [1]. However, with improved imaging parameters and reduced metal artifacts in CT and MR imaging, both are now capable of depicting

* Address for correspondence: Omer Awan, MD, Department of Diagnostic Radiology and Nuclear Medicine, University of Maryland Medical Center, 22 South Greene Street, Baltimore, Maryland 21201, USA.

E-mail address: Omer.awan786@gmail.com (O. Awan).

many complications that arise from THA [3]. CT is useful in detecting early bony changes, including osteolysis and periprosthetic fracture. Large periarticular fluid collections and abscesses can also be seen on CT. Imaging acquisition methods to reduce orthopaedic hardware artifact include using high peak voltage (140 kVp), increasing milliampere seconds (300-450 mAs in adults), narrowing collimation, and using thin sections. Additional ways to reduce artifacts include using a standard or smooth reconstruction algorithm (soft tissue versus bone) and larger reconstruction section thickness.

Metal reduction MR imaging can reveal important periarticular soft-tissue pathology [1]. Metal artifact reduction techniques include using fast spin echo sequences with short echo spacing, small field of view, high-resolution matrix (256 and 512), thin section, and increased frequency-encoding gradient strength. Additional ways to reduce artifact include using lower magnetic field strength as well as positioning the long axis of the prosthesis parallel to the longitudinal axis of the static magnetic field. Short inversion time inversion recovery imaging is less susceptible to magnetic field inhomogeneity and provides more effective fat signal suppression than spectral fat saturation in the presence of orthopaedic hardware.

Early Complications

Dislocation or subluxation of hardware is among the most common complications after THA and can occur both early and late. Reported rates of dislocation range from 0.3%-10% after primary and 10%-28% after revision hip arthroplasty [4]. Most dislocations occur posteriorly, although anterior dislocations also occur. Risk factors for dislocation include trauma and poor muscle tone. Malposition has long been recognized as an important cause of dislocation. Acetabular component anteversion of 15° and abduction of 45° have been described to be associated with the lowest risk of dislocation, although these investigators suggest that there is

not a safe range of position [5]. The type of surgical approach may also contribute to the rate of dislocation. For example, a posterolateral surgical approach is reportedly a greater risk factor than the modified lateral approach [6]. Most dislocations are detected in the immediate postoperative period with radiographs (Figure 1A, B).

Another early complication is malposition of the prosthesis, which is in the same spectrum as dislocation and subluxation, the difference being that, with malposition, the orthopaedic hardware was never initially placed in the appropriate position (ie, the femoral component never articulated with the acetabular component).

Postoperative hematoma is a well-known complication, with a reported incidence of 0%-10% [7]. This potentially devastating complication can result from anticoagulation use as well as a laceration or puncture of a major vessel in the surgical bed. Vessels that may be injured include the iliac and femoral vessels and the profunda femoris, obturator, and superior gluteal arteries. CT by using a non-contrast-enhanced technique is superior to radiographs in diagnosing hematoma (Figure 2A, B). Treatment of hematoma includes intraoperative control via ligation or electrocautery if a specific injured vessel is identified. In addition, applying manual pressure can help control bleeding. Rarely, the patient must return to surgery for evacuation of a postoperative hematoma; the reported incidence of such procedures is 0.24% [8].

Thromboembolic disease, including both deep venous thrombosis and pulmonary embolus, represents the highest risk of perioperative mortality after THA, with the incidence reported to be between 8% and 70%. Perioperative mortality from pulmonary embolus has been reported to be 2%-3% [9]. Anticoagulation, compression stockings, and early ambulation remain standard therapy for everyone undergoing THA. Venogram is the criterion standard, although ultrasonography remains the mainstay for the diagnosis of acute deep venous thrombosis. Furthermore, CT is more often performed to assess for complications associated with THA, and deep

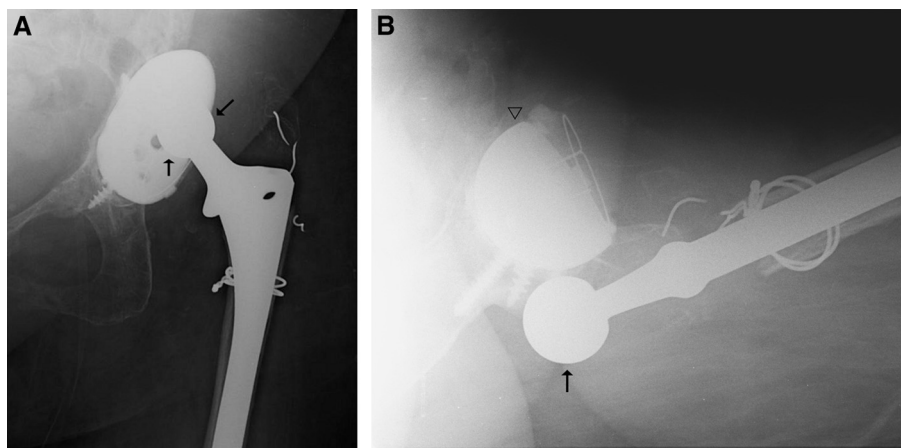


Figure 1. Instability and dislocation. A 43-year-old woman after total hip arthroplasty, who reported dislocation while rolling in bed and reaching for an object. Anterior-posterior (A) and lateral (B) radiographs, showing posterior dislocation of the femoral head (arrows) with respect to a bilobed acetabular cup (arrowhead).

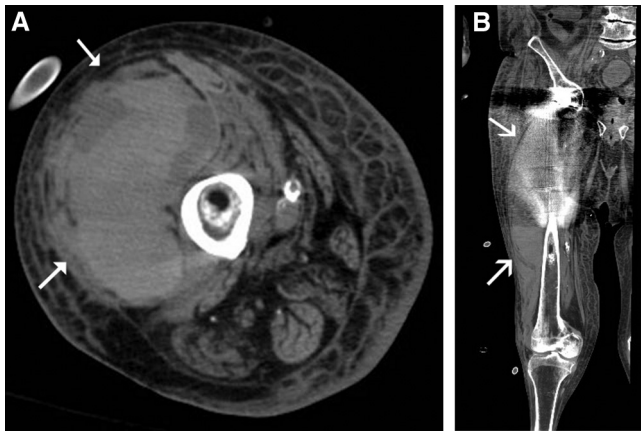


Figure 2. Postoperative hematoma. A 63-year-old man who presented with thigh fullness 1 week after hip arthroplasty. Axial (A) and coronal (B) noncontrast computed tomography images, demonstrating a heterogeneous and predominantly hyperdense mass (arrows) within the vastus muscles consistent with postoperative hematoma.

venous thrombosis can be demonstrated as hypodensity within an enlarged vein during delayed-phase imaging (Figure 3).

Stress shielding results from alterations in stress loading after THA and leads to decreased bone mass and osteoporosis in areas of decreased loading. Stress shielding is typically seen in the greater and lesser trochanters of the femur. Stress shielding is demonstrated on a radiograph as regional demineralization (Figure 4). Stress shielding must be clinically differentiated from infection, and follow-up is important because of the associated risk of pathologic fracture.

Late Complications

Aseptic and mechanical loosening remains the second most common cause of morbidity and revision for patients after THA and accounts for up to 19.7% of all revision

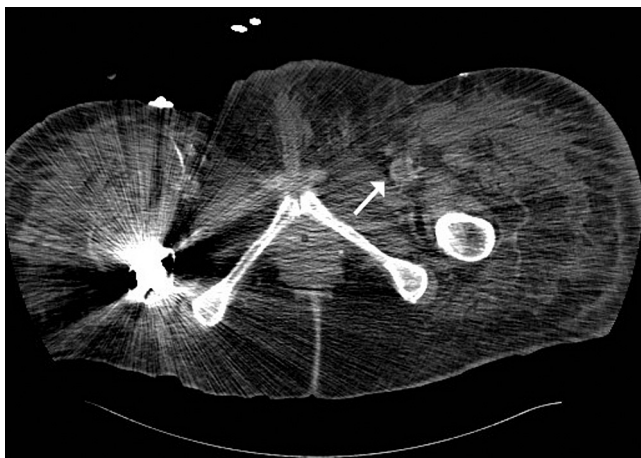


Figure 3. Deep venous thrombosis. A 57-year-old man, who presented with bilateral leg swelling 2 weeks after hip arthroplasty. Axial delayed-phase contrast-enhanced computed tomography image, showing right hip arthroplasty and enlargement of the left iliofemoral vein with hypodensity within the vein, consistent with deep venous thrombosis (arrow).

procedures [4]. Contributing factors to aseptic failure include wear of prosthetic components; poor initial stability of the implant; failure of fixation; and patient factors, such as increased age and weight. Improvements in implant design and surgical technique have led to a decreasing incidence of mechanical loosening, although the overall incidence of this complication is quite variable. Aseptic loosening is often clinically associated with patient pain and discomfort.

The radiographic criteria for diagnosing loosening include periprosthetic radiolucency that is new or >2 mm in diameter, regardless of whether the arthroplasty is cemented or cementless (Figures 5 and 6A) [10]. Additional radiographic signs of aseptic loosening include evidence of prosthesis movement, particularly varus orientation or component rotation, shedding of beads in cementless arthroplasties, and fracture of the cement [10]. The differential diagnosis for periprosthetic radiolucency includes infection and particle disease in addition to aseptic loosening. Radiolucent cement also may demonstrate periprosthetic radiolucency, and revision arthroplasties may have wider radiolucent zones than primary procedures. Thus, a diagnosis of aseptic loosening must be made in conjunction with a clinical history and serial radiographic studies to document change or progression of radiolucency. Although differentiation between aseptic loosening, infection, and particle disease is not always possible with radiography alone, aseptic loosening (Figure 6A, B) tends to produce uniform radiolucency, whereas particle disease produces multifocal radiolucencies related to localized osteolysis. Infection can produce either of these patterns.

Infection has been reported to contribute to 14.8% of all revision THA, the third most common cause after instability and aseptic loosening [4]. Infection can occur during the early and late postoperative periods. Clinical signs and symptoms of fever, pain, and hip discharge and induration, and laboratory tests that included white blood cell counts and erythrocyte sedimentation rate are insensitive and nonspecific. On radiograph (Figure 7A) and CT, diffuse or multifocal osteolysis surrounding the prosthesis (>2 mm or progressive) raises concern for infection; however, this is not always present and can be seen in the setting of aseptic loosening and particle disease.

Soft-tissue abnormalities, including joint distension and fluid collection have been reported to be more reliable in diagnosing infection. CT has been shown to accurately detect these changes (Figure 7B). MR imaging is superior to radiograph and CT in evaluating the soft tissues around the hardware and in demonstrating early fluid collections (Figure 7C, D). Arthrocentesis and synovial biopsy are invasive techniques and may be necessary to diagnose infection. Arthrography alone is usually not specific for the diagnosis but may suggest infection if there are irregularly marginated contrast filling bursae or cavities surrounding the hip [11]. Ultrasound may be useful to assess periarticular fluid collection and guide aspiration.

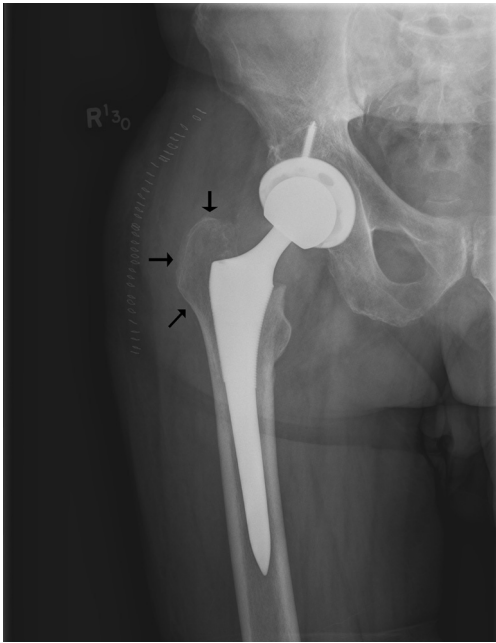


Figure 4. Stress shielding. A 3-week postoperative radiograph after hip arthroplasty in a 63-year-old man, showing localized demineralization of the greater trochanter consistent with stress shielding (arrows).

Given the limited accuracy of diagnostic imaging and invasive nature of routine aspiration, a nuclear medicine scan can serve as an important complement and noninvasive method of evaluating infection [12]. The accuracy of

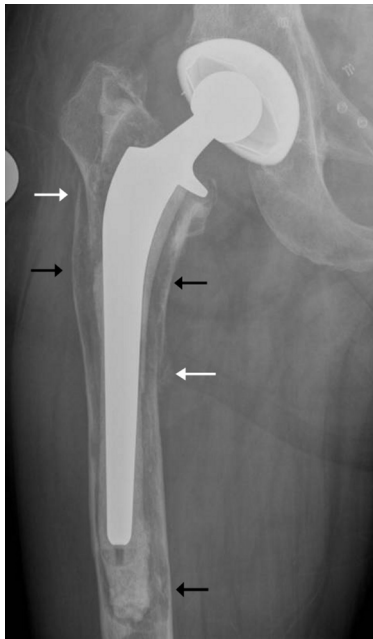


Figure 5. Periprosthetic fracture with underlying mechanical loosening. A 67-year-old man 11 years after total hip arthroplasty for ankylosing spondylitis. He had chronic femoral component loosening and presented 3 weeks after a low-energy fall. Anterior-posterior radiograph, showing diffuse radiolucency suggestive of mechanical loosening at the cement bone interface of the femoral stem (black arrows). A spiral periprosthetic fracture with mild callus formation is secondary to early healing (white arrows).

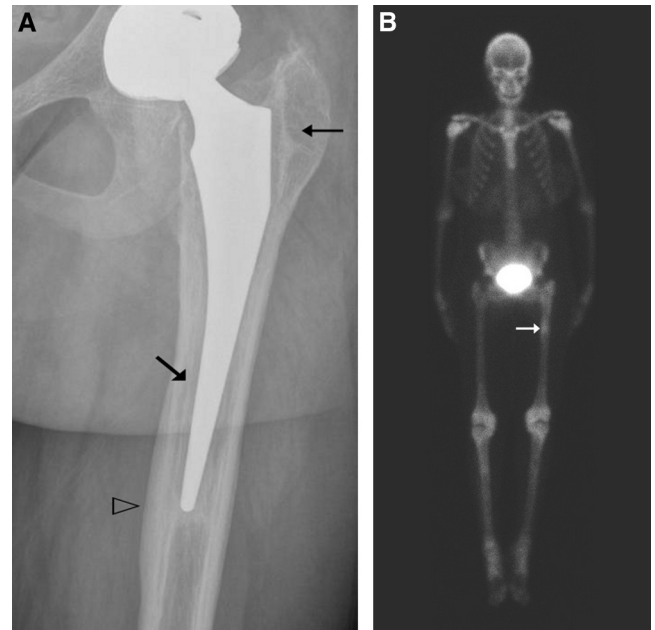


Figure 6. Aseptic mechanical loosening of femoral component. A 58-year-old man with pain 4 years after total hip arthroplasty. (A) Anterior-posterior radiograph, showing radiolucency along both the proximal and distal femoral stem (arrows); reactive cortical thickening is seen in the proximal femur at the level of the distal femoral stem medially (arrowhead). (B) Technetium-99m methylene diphosphonate bone scan, showing increased tracer uptake in this area (arrow).

combined leukocyte-marrow imaging of 90% is the highest among nuclear medicine studies. The labeling of inflammatory cells that migrate to the sites of infection is useful in detecting the neutrophil-mediated inflammatory process and can distinguish between the inflamed and the aseptically loosened prosthesis. Background bone marrow assessment is accomplished by using technetium-99m sulfur colloid. Because both labeled leukocytes and sulfur colloid accumulate in the bone marrow, but only labeled leukocytes accumulate in infection, activity on labeled leukocyte images without activity on the sulfur colloid images is accurate in diagnosing infection 90% or more of the time.

Periprosthetic fracture is a rare complication, with an incidence of <1% after THA [4]. This fracture is typically related to loosening, stress shielding, or trauma (Figure 5). The Vancouver classification system is often used to classify these fractures [13]. A type A fracture is located in the trochanteric region, a type B fracture is located about the stem or the tip of the stem, and a type C fracture is well distal to the tip of the stem. Treatment options for periprosthetic fractures include nonoperative management with protected weight bearing, revision arthroplasty, or internal fixation [14]. Treatment options depend on bone quality, patient age, limb alignment, fracture pattern, and stability of the implant.

Particle disease and histiocyte response results from macrophage reaction to various parts of the arthroplasty. This complication typically occurs between 1 and 5 years after initial surgery and is a major cause of periprosthetic radiolucency on postoperative radiographs (Figure 8A). Although



Figure 7. Infection. (A, B) A 49-year-old man with persistent pain, erythema, fever, leukocytosis, and elevated erythrocyte sedimentation rate and c-reactive protein 4 months after right hip arthroplasty. (A) Radiograph, showing demineralization, predominantly of the right greater and lesser trochanters (arrows). (B) Axial computed tomography, showing a sinus tract extending from the hip joint towards the skin surface, consistent with infection (arrows). (C, D) A 54-year-old man presented 15 years after right hip arthroplasty. Sagittal (C) and axial (D) short tau inversion recovery magnetic resonance imaging (repetition time/echo time, 6000 ms/62 ms) with metal artifact reduction technique, demonstrating focal fluid signal collection posterior to the hip arthroplasty in this patient with fever and leukocytosis, findings compatible with early abscess formation confirmed with subsequent aspiration (arrows). Note the soft-tissue oedema surrounding the fluid collection. This fluid collection is posterior and may not have been correctly diagnosed by joint aspiration via the anterior approach.

particles from any of the components of the prosthesis can induce a histiocyte response, debris from polyethylene wear is most commonly responsible [15]. Radiographic signs of particle disease can be subtle and confused with infection and aseptic loosening. However, endosteal scalloping is more characteristic of particle disease. Particle disease is often better depicted on CT, with which the macroparticles within the joint may be seen (Figure 8B, C).

Metallosis/pseudotumour/aseptic lymphocyte-dominated vasculitis-associated lesions is another potential complication after THA. Second-generation metal-on-metal arthroplasty was introduced in the early 1990s to reduce the rate of THA failure associated with polyethylene wear. More recent clinical studies have implicated metal hypersensitivity as a mechanism of aseptic failure after these arthroplasties [16]. Serum levels of cobalt and chromium ions are

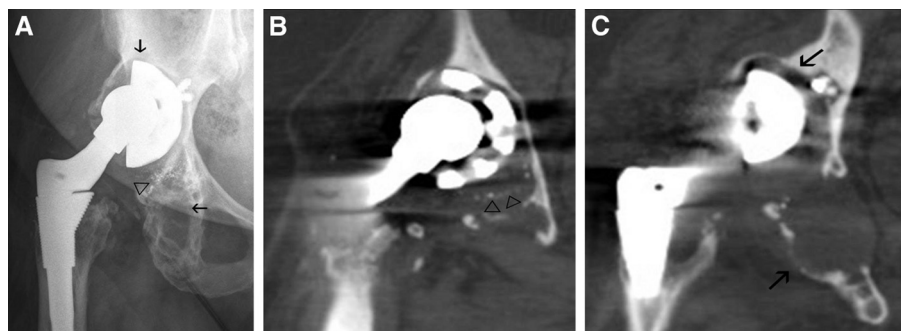


Figure 8. Particle disease and histiocyte response. A 51-year-old woman with a history of total hip replacement for Perthes disease at a young age, presenting with right hip pain and restricted range of motion. Anterior-posterior radiograph (A) and coronal computed tomography images (B, C) of the right hip, demonstrating acetabulum component loosening with vertical orientation of the acetabulum cup and surrounding osteolysis (arrows). Punctate high-density foci are present within the area of osteolysis (arrowheads).

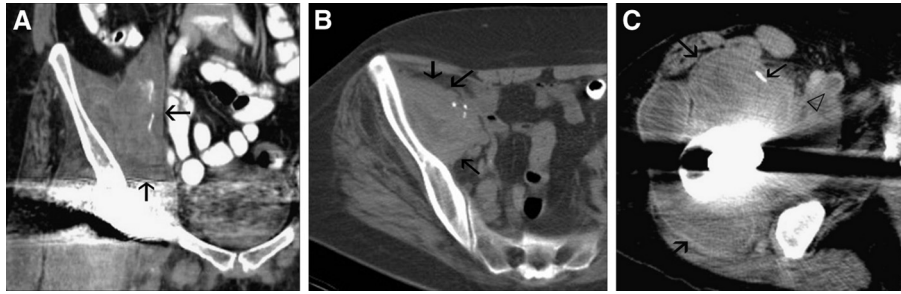


Figure 9. Metallosis/pseudotumour/aseptic lymphocyte-dominated vasculitis-associated lesions. A 68-year-old woman with a history of right metal-on-metal hip arthroplasty presented with right leg pain and swelling. A radiograph was unrevealing (not shown). Her blood cobalt level was markedly elevated, at 42 ng/mL (reference range, 0.0–0.9 ng/mL) and chromium at 14 ng/mL (reference value, <0.3 ng/mL). She had no fever or leukocytosis. Coronal (A) and axial (B, C) computed tomography images, showing a large heterogeneous density mass extending in the right iliopsoas and right thigh muscles with internal foci of radiodensities (arrows). In addition, thrombus is identified within the right iliofemoral vein (arrowhead). Pathologic analysis showed extensive fibrohistiocytic reaction with foreign material consistent with metallosis. Soft tissue and bone necrosis is present. No malignancy was seen.

substantially higher in individuals with THA than in individuals without THA. Released metal ions can activate the immune system by forming metal-protein complexes that can elicit hypersensitivity responses. Imaging can show periprosthetic osteolysis or pseudotumours associated with metal hypersensitivity wear (Figure 9A–C). On the histologic level, the process involves cobalt-chromium metallosis, tissue necrosis, and a predominant perivascular lymphoplasmacytic infiltrate [16]. Pseudotumour has been described as a rapidly growing lesion that resembles tumour, with extensive bone loss, neither infective nor neoplastic, caused by excessive wear debris in the vicinity of a THA. No clear consensus exists in defining the boundaries of the terms metallosis, aseptic lymphocyte-dominated vasculitis-associated lesions, and pseudotumours.

Heterotopic ossification has been reported to occur in up to 39% of patients after THA. Patients typically present with hip stiffness. Histologically primitive mesenchymal cells in the surrounding soft tissues are transformed into

osteoblastic tissue, which then forms mature lamellar bone. Detectable calcific density can be seen on radiographs and CT within weeks after surgery, with ankylosis seen as early as 12 weeks after surgery [17] (Figure 10). A 3-phase bone scan is the most sensitive imaging modality in the early phase of heterotopic ossification. The flow and blood-pool phase images can show increased tracer uptake approximately 2.5 weeks after injury, 1 week before a bone scan becomes positive, and 1–4 weeks before radiographic detection [18].

The most widely accepted classification system of heterotopic ossification was postulated by Brooker et al [19] and is classified into 4 grades. Grade I heterotopic ossification represents islands of bone within soft tissues around the hip; grade II includes bone spurs that arise from the pelvis or the proximal end of the femur, leaving ≥ 1 cm between opposing bone surfaces; grade III is similar to grade II except that the distance is <1 cm; and grade IV represents radiographic ankylosis. Early treatment typically consists of either radiotherapy or the use of nonsteroidal anti-inflammatory medication, whereas more advanced heterotopic ossification may necessitate surgical resection [20].

Pseudobursa formation, which typically can be detected by arthrography or cross-sectional imaging, represents irregular recesses that communicate with the joint (Figure 11A–D). This finding can be noted incidentally and may or may not be associated with infection. Arthrocentesis may be performed to rule out infection, although more subtle findings that may indicate infection include irregular pseudobursa walls, osteolysis, and sinus tracts. Correlation with clinical presentation is a requirement. Uninfected pseudobursa may be treated with either steroid or anesthetic injections.

Conclusion

The combination of radiographic and advanced imaging techniques allows for accurate interpretation of complications associated with hip arthroplasty. Although radiographs remain essential in initial evaluation of the postoperative

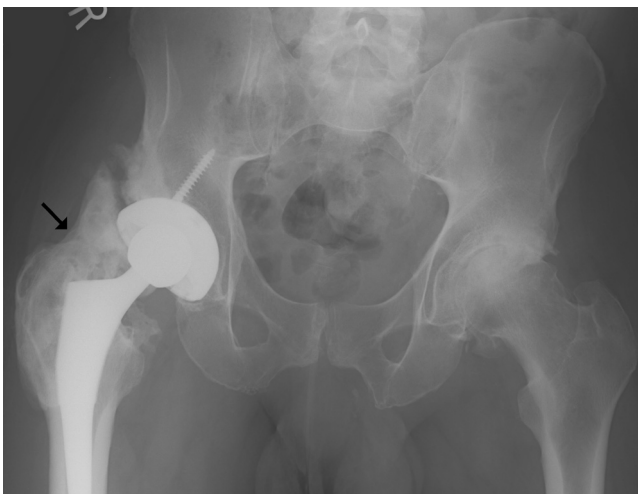


Figure 10. Heterotopic ossification. A 45-year-old man, who presented >2 years after total hip arthroplasty with restricted range of motion. Anterior-posterior radiograph, showing severe heterotopic ossification nearly bridging the right greater trochanter and the acetabulum (arrow).

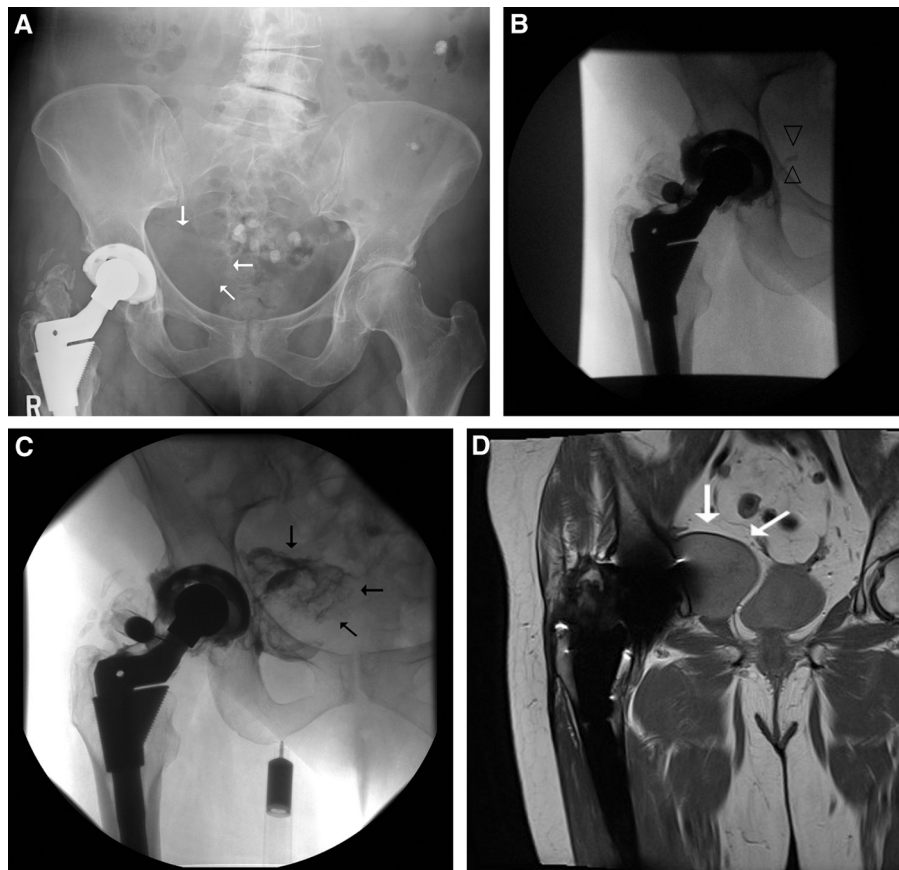


Figure 11. Pseudobursa. A 64-year-old man presented with fullness around the hip 4 years after total hip arthroplasty. Routine 1-year postoperative anterior-posterior radiograph (A), showing moderate heterotopic ossification. Computed tomography abdomen and pelvis performed to evaluate epigastric pain showed a mass in the right pelvis (not shown). Retrospective review of this radiograph, showing a soft-tissue density in the right pelvis (arrows). Joint aspiration yielded no fluid. (B) Arthrogram initially showed a thin tract extending towards the pelvis (arrowheads). (C) With additional injection of contrast, filling of a right pelvic fluid collection (arrows) is seen. (D) Magnetic resonance imaging, fast spine echo proton density (TR/TE, 1870 ms/28 ms) by using the metal-reduction technique, showing the smooth and thin rim of this fluid collection (arrows) and confirmed that no additional fluid collection was present.

patient, arthrography, ultrasound, and nuclear medicine can provide complement in assessing periarticular fluid collections and infection. CT can better demonstrate osteolysis, fracture, abscess, and hematoma. MR imaging is useful in evaluating soft-tissue abnormalities.

References

- [1] White LM, Kim JK, Mehta M, et al. Complications of total hip arthroplasty: MR imaging-initial experience. *Radiology* 2000;215:254–62.
- [2] Cushner F, Agnelli G, FitzGerald G, et al. Complications and functional outcomes after total hip arthroplasty and total knee arthroplasty: results from the Global Orthopaedic Registry. *Am J Orthop* 2010;39(suppl):22–8.
- [3] Lee MF, Kim S, Lee SA, et al. Overcoming artifacts from metallic orthopedic implants at high-field-strength MR imaging and multi-detector CT. *RadioGraphics* 2007;27:791–803.
- [4] Bozic KJ, Kurtz SM, Lau E, et al. The epidemiology of revision total hip arthroplasty in the United States. *J Bone Joint Surg Am* 2009;91:128–33.
- [5] Biedermann R, Tonin A, Krismer M, et al. Reducing the risk of dislocation after total hip arthroplasty: the effect of orientation of the acetabular component. *J Bone Joint Surg Br* 2005;87:762–9.
- [6] White Jr RE, Forness TJ, Allman JK, et al. Effect of posterior capsular repair on early dislocation in primary total hip replacement. *Clin Orthop Relat Res* 2001;393:163–7.
- [7] Silvia M, Luck Jr JV. Long-term results of primary total knee replacement in patients with hemophilia. *J Bone Joint Surg Am* 2005;87:85–91.
- [8] Galat DD, McGovern SC, Hanssen AD, et al. Early return to surgery for evacuation of a postoperative hematoma after primary total knee arthroplasty. *J Bone Joint Surg Am* 2008;90:2331–6.
- [9] Haas SB, Barrack RL, Westrich G. Venous thromboembolic disease after total hip and knee arthroplasty. *Instr Course Lect* 2009;58:781–93.
- [10] Tigges S, Stiles RG, Roberson JR. Complications of hip arthroplasty causing periprosthetic radiolucency on plain radiographs. *AJR Am J Roentgenol* 1994;162:1387–91.
- [11] Roberts P, Walters AJ, McMinn DJ. Diagnosing infection in hip replacements. The use of fine-needle aspiration and radiometric culture. *J Bone Joint Surg Br* 1992;74:265–9.
- [12] Love C, Tomas MB, Marwin SE, et al. Role of nuclear medicine in diagnosis of the infected joint replacement. *Radiographics* 2001;21:1229–38.
- [13] Duncan CP, Masri BA. Fractures of the femur after hip replacement. *Instr Course Lect* 1995;44:293–304.
- [14] Springer BD, Berry DJ, Lewallen DG. Treatment of periprosthetic femoral fractures following total hip arthroplasty with femoral component revision. *J Bone Joint Surg Am* 2003;85:2156–62.

- [15] Carty FL, Cashman JP, Parvizi J, et al. Imaging of the postoperative hip. *Semin Musculoskelet Radiol* 2011;15:357–71.
- [16] Rajpura A, Porter ML, Gambhir AK, et al. Clinical experience of revision of metal-on-metal hip arthroplasty for aseptic lymphocyte dominated vasculitis associated lesions (ALVAL). *Hip Int* 2011;21:43–51.
- [17] Weissman BNW, Sledge CB. The hip. In: Weissman BNW, Sledge CB, editors. *Orthopedic Radiology*. Philadelphia: WB Saunders; 1991. p. 385–495.
- [18] Shehab D, Elgazzar AH, Collier BD. Heterotopic ossification. *J Nucl Med* 2002;43:346–53.
- [19] Brooker AF, Bowerman JW, Robinson RA, et al. Ectopic ossification following total hip replacement. Incidence and a method of classification. *J Bone Joint Surg Am* 1973;55:1629–32.
- [20] Chao ST, Joyce MJ, Suh JH. Treatment of heterotopic ossification. *Orthopedics* 2007;30:457–64.

Book Review / Critiques de livres

Book Review: MRI Made Easy (for Beginners), 2nd ed. Govind B. Chavhan. Ashland, OH: JP Medical Publishers Ltd; 2013, 208 pages, CAD\$44.00. ISBN: 978-93-5090-270-7

MRI Made Easy is an introductory textbook that aims to provide a basic overview of the fundamentals that pertain to this imaging modality. This is the second edition of the text, the first of which was published in 2007. The first edition was well received by medical students and junior residents because it provided a palatable jumping point for conquering the modality as a whole. The second edition has now expanded to include recently developed sectors of MRI, including the following: 3-Tesla magnetic resonance imaging (MRI), susceptibility weighted imaging, magnetic resonance (MR) enterography, and MR urography. Furthermore, previous chapters on clinical applications of sequences have been revised to now include rationales for their usage, a significant improvement from the first edition, which simply listed their applications. This second edition, therefore, hopes to expand upon its predecessor while maintaining simplicity for its target audience.

This book contains 21 chapters, with a total of 208 pages, and it is divided into 2 sections. The first section, of 12 chapters, outlines basic principles, scanning parameters, accessory techniques, system instrumentation, sequences, artifacts, and basic interpretation principles. The second section delves into higher applications of MRI, such as 3-Tesla MRI, MR angiography, diffusion, perfusion, spectroscopy, cardiac imaging, cholangiopancreatography, and other miscellaneous applications.

MRI Made Easy, although brief, is well written and uses images and diagrams in an effective manner. The MRIs are of good quality, with well-written captions to help guide a beginner through the findings. Furthermore, the author has provided numerous summary charts throughout the text that are well constructed and act as valuable learning tools. The first section, which introduces the reader to MR theory and basic principles, is particularly useful for those with little to no exposure to MRI. The author is commended on his ability to simplify material and present it in an easy-to-digest manner. As expected from such a brief textbook, the diagnostic findings and pathologies outlined in the second half of the book are superficial and somewhat limited. Nevertheless, the author was successful in scratching the surface of the vast majority of pertinent topics while producing a textbook that can be read with ease in an afternoon.

Furthermore, this textbook has been made in a useful size and could easily fit in one's pocket or white coat, a near necessity for the current-day student. Finally, the textbook contains a CD-ROM, which provides the reader with an online version of the images found in the book. Although this may be of use to some readers, the fact that no supplementary images were provided was a disappointing discovery. Given the relatively limited focus on MRI anatomy in this textbook, future editions may consider adding this content to the CD-ROM. This CD-ROM also was found to be solely compatible with Windows Operating Systems (Microsoft Corp, Redmond, WA), thus limiting its universal utility.

MRI Made Easy certainly lives up to its expectation and is particularly useful for medical students or junior residents outside of diagnostic radiology. Given the superficial coverage of specific diagnostic findings and pathology, it would likely be of limited use to radiology trainees or radiologists. That being said, this textbook undoubtedly has a useful role in early medical education.

There are a number of similar textbooks that provide a basic approach to MRI. Two of the most positively reviewed textbooks include *MRI: The Basics* by Hashemi et al. (Lippincott Williams & Wilkins, Philadelphia, PA, 2010) and *MRI: Basic Principles and Applications* by Brown et al (Wiley-Blackwell, Hoboken, NJ, 2010). Both textbooks, however, are more costly and do not cover the same breadth of topics. Given the price of \$44.00, *MRI Made Easy* should be considered by any medical student who wishes to expand his or her knowledge base.

This textbook, although superficial, provides a strong knowledge base for those with little to no MRI exposure. Given that it is well written, uses many images and tables as learning aides, and adequately expands upon its successful first edition, this textbook will likely prove to be widely read.

Tyler M. Coupal, BMSc
Michael G. DeGroot School of Medicine
McMaster University
E-mail address: tyler.coupal@medportal.ca

Peter L. Munk, MD
Editor in Chief, CARJ
Professor of Radiology
University of British Columbia
Vancouver, BC, Canada